INDONESIAN JOURNAL ON GEOSCIENCE
Geological Agency
Ministry of Energy and Mineral Resources

Journal homepage: http://ijog.geologi.esdm.go.id
ISSN 2355-9314, e-ISSN 2355-9306

The Magnetostratigraphy and the Age of So'a Basin Fossil-Bearing Sequence, Flores, Indonesia

Dida Yurnaldi, Ruly Setiawan, and Emma Yan Patriani

Centre for Geological Survey, Geological Agency
Jln. Diponegoro no 57 Bandung - 40122

Corresponding author: dyurnaldi@yahoo.com
Manuscript received: November, 07, 2017; revised: January, 08, 2018;
approved: June, 05, 2018; available online: November, 19, 2018

Abstract - Three fossil-bearing intervals have been recognized in the Pleistocene So'a Basin, with the upper one holding important evidence of hominin fossils. The sequence also contains numerous *in situ* stone artifacts and fossils of other vertebrate taxa. Therefore, multiple dating techniques are crucial to secure the age of the fossil and artifact-bearing layers, especially the one with the hominin remains. This paper deals with the palaeomagnetic dating of the So'a Basin sequence to assist other dating methods that have been applied, and to refine the chronostratigraphy of the area. Palaeomagnetic sampling was conducted in four sections along a west to east transect. Four magnetozones can be recognized, consisting of two reverse and two normal polarity zones. By using the available radiometric ages as a guide and comparing the So'a Basin magnetostratigraphy with the Standard Geomagnetic Polarity Time Scale (GPTS), it became clear that both reverse magnetozones are part of the Matuyama Chron, while the normal magnetozones are the Jaramillo subchron and the Brunhes Chron. These palaeomagnetic dating results support the available radiometric dates and refine the age of the fossil-bearing deposits of the So'a Basin.

Keywords: Palaeomagnetic, *Homo floresiensis,* hominin, dating, polarity, rock magnetics

How to cite this article:
Yurnaldi, D., Setiawan, R., and Patriyani, E.Y., 2018. The Magnetostratigraphy and the Age of So'a Basin Fossil-Bearing Sequence, Flores, Indonesia. *Indonesian Journal on Geoscience*, 5 (3), p.221-234. DOI: 10.17014/ijog.5.3.221-234

Introduction

Recently, a mandible fragment and six hominin teeth were recovered from one of the fossil-bearing strata in the So'a Basin, Flores, Indonesia. These specimens are relatively similar to the holo-type of *Homo floresiensis* from Liang Bua, except the size which is slightly smaller and the mandibular first molar that has more primitive characteristics than the Liang Bua specimens (van den Bergh *et al.,* 2016a; see also Brown and Maeda, 2009).

Multiple dating methods were applied to determine the age of these important hominin fossils, which are estimated to be c. 700,000 years old (Brumm *et al.*, 2016). In order to refine the chronostratigraphy of the So'a Basin sequence and to allow basin-wide cross correlation, palaeomagnetic sampling and analysis were carried out on four stratigraphic sections. The combination of palaeomagnetic dating and other radiometric dating techniques has widely been used and proven to be successful for dating archaeo- and palaeontological sites around the world, for example: the Koobi Fora site (Lepre and Kent, 2010), Sterkfontein Cave (Herries *et al.*, 2010), and the Melka Kunture site (Tamrat *et al.*, 2014)

in Africa, the Ceprano- Fontana Ranuccio site (Muttoni *et al.*, 2009) and the Poiana Cireşului site in Europe (Zeeden *et al.*, 2009), and the Nihewan Basin (Zuo *et al.*, 2011; Ao *et al.*, 2013) in Asia. In Indonesia, palaeomagnetic dating was used to date the Sangiran site in Java (Hyodo *et al.*, 1993; 2011) and The Talipu site in Sulawesi (van den Bergh *et al.*, 2016b). Magnetostratigraphy was applied to better constrain of the numeric ages and to complement other dating methods, including Fission-Track, Argon-Argon, Electron Spin Resonance, and optical dating techniques.

Geological, Palaeontological, and Geochronological Context of The So'a Basin

The So'a Basin is located in the central part of Flores, almost entirely surrounded by mountains and active volcanoes (Figure 1). It is drained by the Ae Sissa River, which empties the basin through a deeply incised gorge to the northeast, and forms a delta plain on the north coast (O'Sullivan *et al.*, 2001; Suminto *et al.*, 2009). The basin basement consists of the Ola Kile Formation comprising massive and resistant andesitic breccias interbedded with minor tuffaceous siltstones, sandstones, and lava flows. It had been tilted by tectonic activity which dips up to 5° to the south (Hartono, 1961; O'Sullivan *et al.,* 2001; Suminto *et al.,* 2009). The Ola Bula Formation unconformably overlies the Ola Kile Formation and fills much of the basin with an up to 100 m thick sequence. It consists of relatively undisturbed and horizontally bedded volcanic and sedimentary deposits, which started to infill the basin during the Late Pliocene or Early Pleistocene (Murouka *et al.*, 2002; Suminto *et al.*, 2009). The Ola Bula Formation is divided into three lithological members, from old to young: the Tuff Member, the Sandstone Member, and the Limestone Member (Hartono, 1961; van den Bergh, 1999; and Suminto *et al.*, 2009 - Figure 2).

Three main fossil-bearing intervals have been recognized within the Ola Bula sequence. The oldest fossiliferous layers are developed within the Tuff Member, which has its most complete development near the Tangi Talo site in the central and deepest part of the basin. The fossil fauna from this level consists of a dwarfed extinct elephant (*Stegodon sondaari*), a giant tortoise, and *Varanuskomodoensis*, but the site has not yielded any stone artifact (Sondaar *et al.*, 1994; Aziz *et al.,* 2009). Two fossil intervals higher up in the sequence lie within the Sandstone Member and can be found at the Mata Menge site. Both

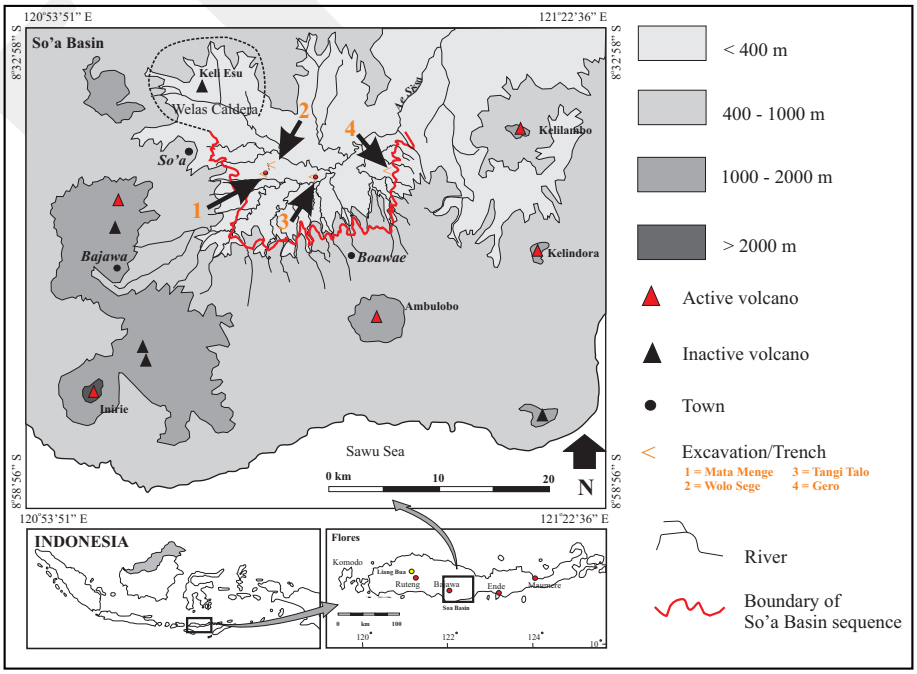

Figure 1. The four site locations of the So'a Basin that were sampled for this study (map modified after van den Bergh, 2010).

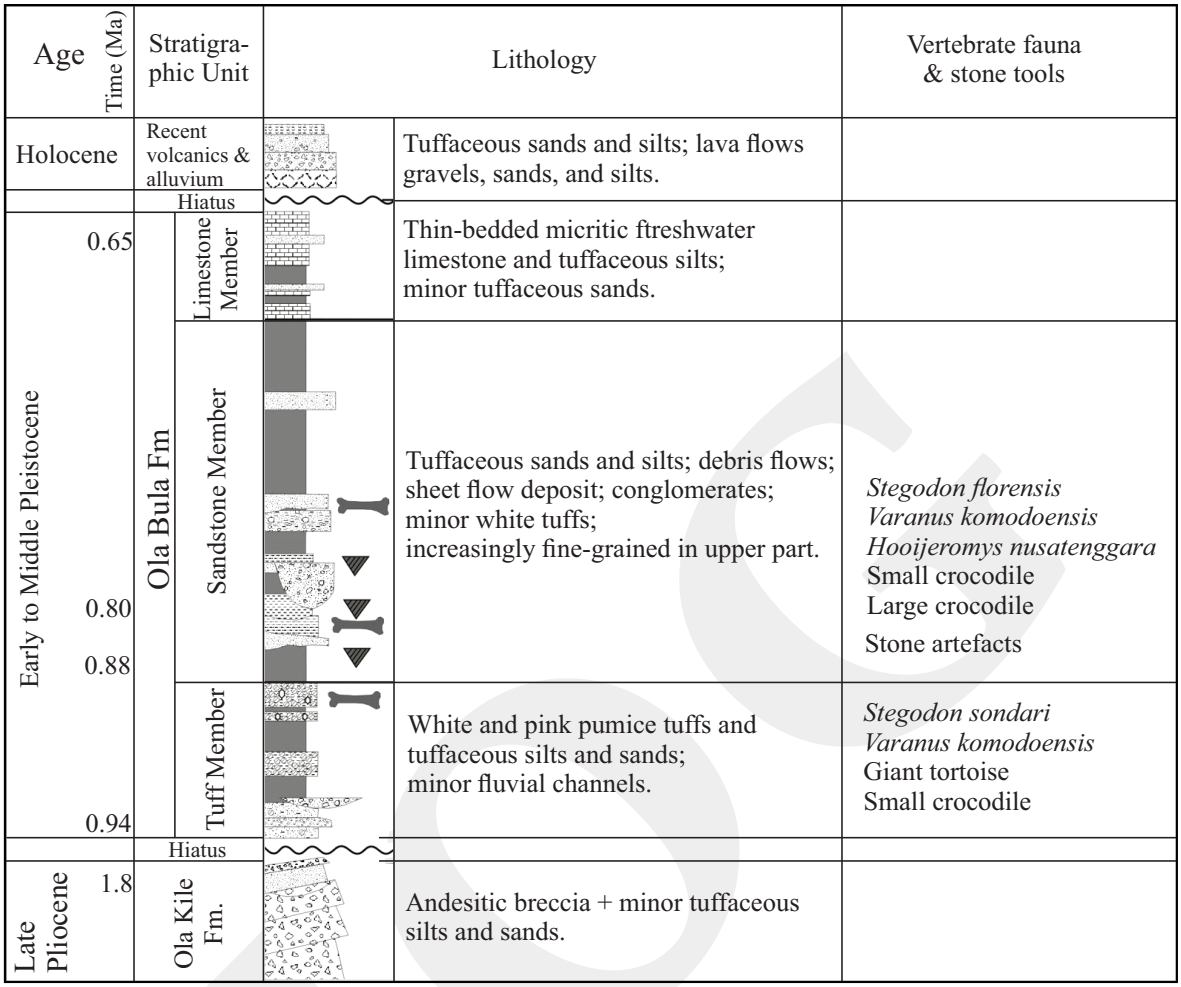

Figure 2. Generalized lithostratigraphy of the So'a Basin (after Suminto *et al.*, 1999).

levels contain the remains of a larger Stegodon (*Stegodon florensis*), a giant rat (*Hooijeromys nusatenggara*), Komodo dragon (*Varanus komodoensis*), unidentified crocodilian remains, and stone artifacts (Sondaar *et al.*, 1994; van den Bergh 1999; van den Bergh *et al.*, 2009; Brumm *et al.*, 2016). In addition, the upper level has yielded the remains of a small-sized hominin, and thought to be the ancestral form of *Homo floresiensis* (van den Bergh *et al.,* 2016).

Dates have come from multiple methods. Previously, the Tangi Talo fossil assemblage was estimated to be 0.9 Ma old based on palaeomagnetic and fission track dating (Sondaar *et al.,* 1994; Morwood *et al.*, 1998). More recently, $^{40}Ar/^{39}Ar$ dating by Brumm *et al.* (2010) of a widespread ignimbrite marker bed yielded an age of ~1.02 ma. This Wolo Sege ignimbrite (WSI) can be recognized throughout the basin, including at the Tangi Talo site, where it occurs at ~20 m above the Tangi Talo fossil bearing layer. Therefore, the Tangi Talo fossil bearing layer could be much older than ~0.9 Ma.

In 2016, the Mata Menge two fossil-bearing layers have been dated as well. Both fossil intervals occur above the WSI, indicating that they must be younger than ~1.02 Ma. Ages of the lower fossil interval lie between ~0.88 Ma and ~0.8 Ma, based on the fission-track dating of two sampled levels, one directly below and one associated with the fossil bearing layer (O'Sullivan *et al.*, 2001). The upper fossil-bearing interval, containing hominin remains, has an age estimate based on its stratigraphic position, because no direct dating associated with this sedimentary layer. The hominin layer occurs 12.5 m above the level that yielded the F-T

date of ~0.8 Ma and 13.5 m below a tephra layer dated at ~0.65 Ma by means of $^{40}Ar/^{39}Ar$ dating, and another primary tephra layer occurring at the top of the Mata Menge section has been $^{40}Ar/^{39}Ar$ dated at ~0.51 Ma (Brumm *et al.*, 2016). In addition, there are also U-series ages of a hominin tooth root fragment and combined U-series and electron spin resonance (ESR) dates of two *S. florensis* molars that were found *in situ* in the same layer as the hominin fossils. The U-series dating yield a minimum age of at least 0.55 Ma, whereas the combined U-series/ESR dating indicates minimum ages around 0.36 Ma and 0.69 Ma, respectively (Brumm *et al.*, 2016). Based on those dates above, Brumm *et al.* (2016) concluded that the hominin fossil layer is estimated to be ~0.7 Ma old.

Materials and Methods

At least six to eight hand specimens were taken from each of twenty-nine clay and/or silt layers from the baulks of four step trenches in the So'a Basin. Sampling was done by carving fresh sediment surfaces to fit into 8 cm^3 acrylic cubes. Orientation of the samples followed the procedure of Tauxe (2003), with a little modification where the laboratory arrow is the same as the specimen strike arrow. Additional non-oriented samples were also taken from each layer for rock magnetic analysis.

Natural Remanent Magnetization (NRM) was measured using 2G a three-axis cryogenic magnetometer from William S. Goore, Inc. (WSGI). Specimens were stepwise demagnetized using an alternating field (AF) with increment intervals of 0.5 - 2.5 mT up to 100 mT. A duplicate thermal demagnetization (TD) was also used on each 'twin' specimen. However, most of the TD decay pattern was found to be erratic and hard to interpret. Rock magnetic parameters were measured using a Princeton Micromag 3900 series Vibrating Sample Magnetometer (VSM). All analyses were performed in a magnetic field-free room at the Palaeomagnetic Laboratory of the Australian National University (ANU) Canberra.

Magnetic minerals were extracted from 10 g samples dispersed in 80 ml distilled water using a magnetic stirrer for SEM-EDX purposes. SEM-EDX analysis was performed using a JEOL-JSM 636OLA at the Geological Laboratory of the Centre of Geological Survey of Indonesia.

Magnetic mineral domains were determined using Dunlop plot (Dunlop *et al.*, 2002). The Characteristic Remanent Magnetization (ChRM) was analyzed using Zijderveld diagrams (Zijderveld, 1967) and Principal Component Analysis (PCA; Kirschvink, 1980) with Puffin Plot software (Lurcock and Wilson, 2012). The direction of ChRMs was determined from orthogonal plots in at least four to five successive measurement steps with the maximum angular deviation (MAD) setting at <15º. The group mean direction was analyzed using Fisher statistics (Fisher, 1953) in IAPD 2000 software. For reversal tests, the method of McFadden & McElhinney (1990) and Butler (1998) was followed using PMAGTOOL v 4.2 by Hounslow (2006). One issue that must be taken into account is that low latitude areas have a relatively weak geomagnetic force as compared to middle and high latitudes, especially with regard to the vertical component (Shimizu *et al.*, 1985). Kobayashi *et al.* (1971) have found that near the equator, the inclination (vertical component) has large fluctuations, so that it is not suitable to use it for tracing geomagnetic reversals. On the other hand, it is also noted that the declination (horizontal component) shows sharp shifts at the reversals.

Result and Disscussion

The Carrier of the Magnetization

A Dunlop plot (see Figure 3) shows that the magnetization carriers consist of a mix of single- and multidomain (SD-MD) grains, with a dominance of MD grains of up to 60 – 90 %. Some of the grain plots show a shift to the SD and superparamagnetic (SP) mix curve, which indicates that SP components also occur in some samples. During demagnetization most of the intensities are reduced to 10 % from the total intensity prior to demagnetization, at relatively low AF peaks of 30-50 mT (Figure 4). Above 50 mT, most specimens are demagnetized completely.

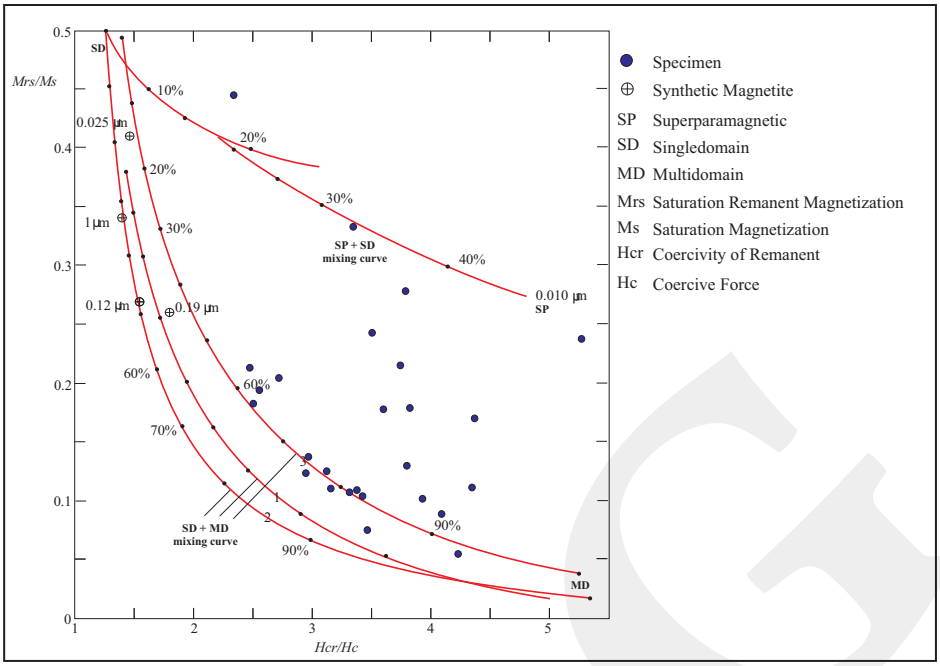

Figure 3. Hysteresis data for samples from So'a Basin, compared to theoretical model curves by Dunlop (2002). Percentages along mixing curve are the proportion of grain.

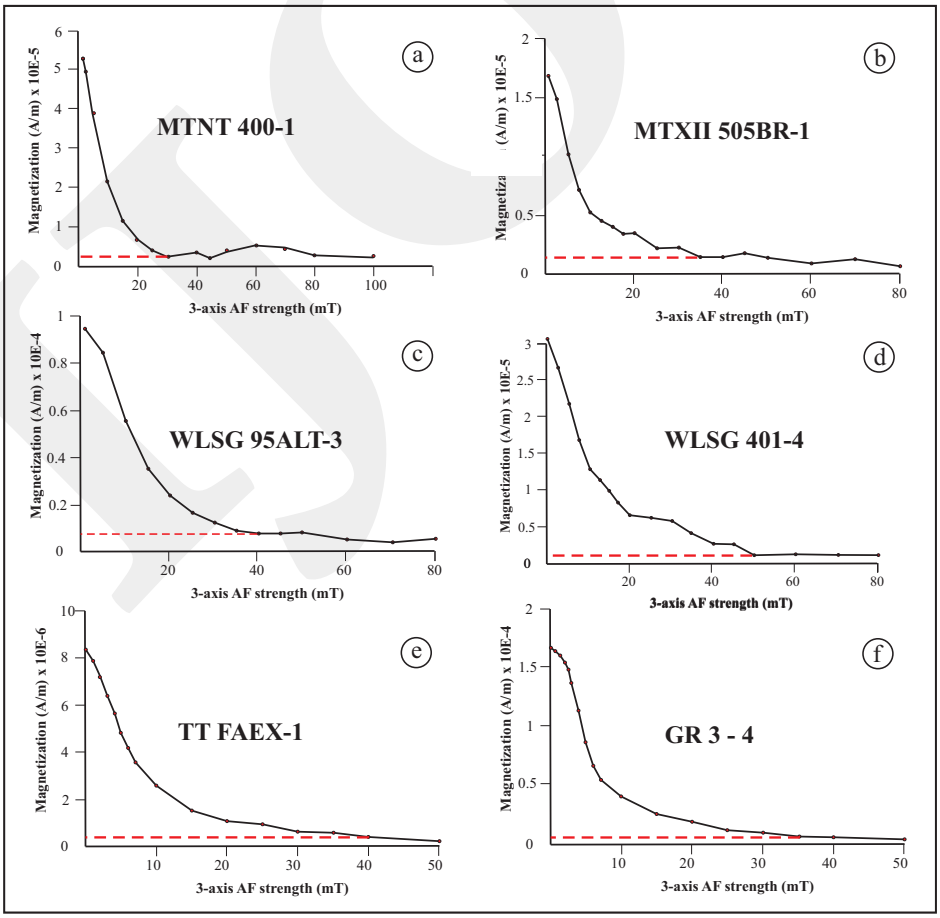

Figure 4. Typical of progressive demagnetization curves of samples from Mata Menge (a, b), Wolo Sege (c, d), Tangi Talo (e), and Gero (f).

This indicates that the carriers of the magnetization are dominated by low coercivity minerals, such as magnetite and/or titanomagnetite. The typical tall and thin hysteresis loops also reflect the occurrence of magnetite and/or titanomagnetite (Figure 5), although such profiles can also rise from the combination of magnetic minerals with contrasting coercivities (Roberts *et al*., 1995).

However, SEM-EDX was able to confirm that the carriers of the magnetization likely represent MD titanomagnetite (Figure 6). This would explain why the thermal demagnetization (TD) did not work, because it is not suitable for the magnetization with magnetite carrier (McElhinney, 2000).

The Characteristics Remanent Magnetization (ChRM)

Most magnetization vectors obtained from all specimens show two to three separated components of NRM on the orthogonal planes (Figure 7). This means that these specimens were affected by a secondary magnetization. However,

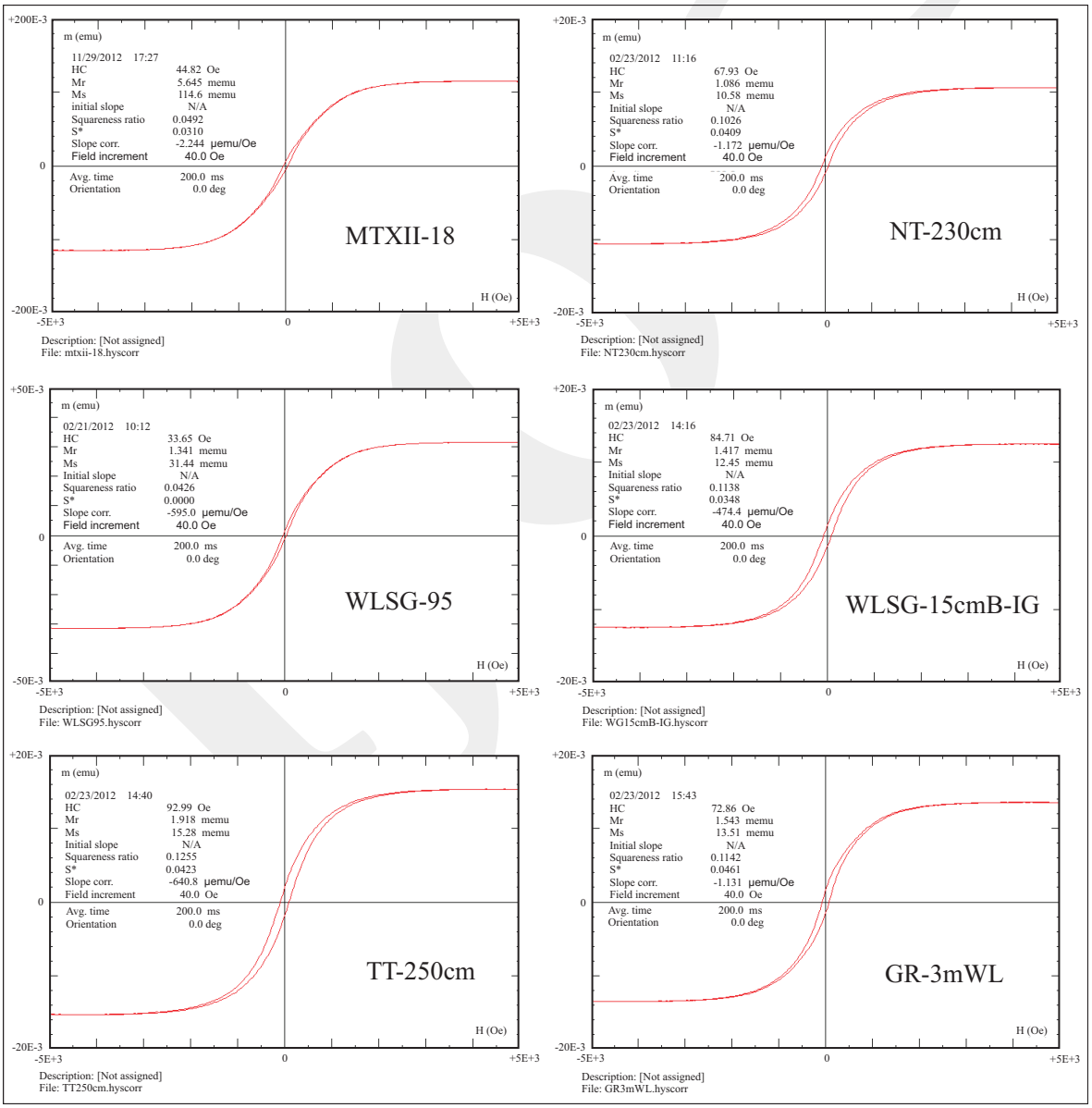

Figure 5. Typical hysteresis loop curves from Mata Menge (top), Wolo Sege (middle), Tangi Talo (lower left), and Gero (lower right). The wasp-waisted curves represent typical hysteresis loops for mixed magnetic mineral assemblages dominated by magnetite.

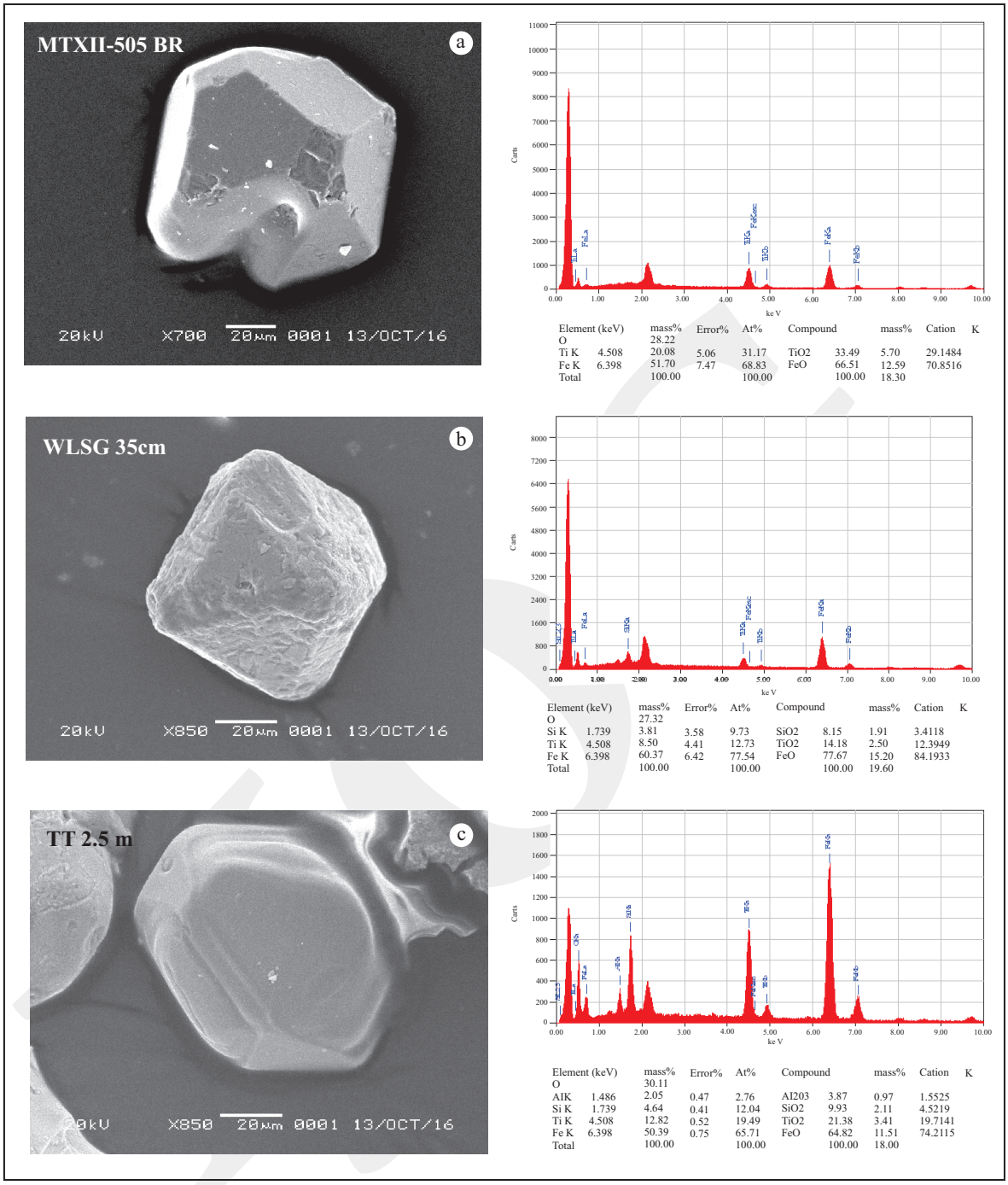

Figure 6. SEM images of representative samples from Mata Menge (a), Wolo Sege (b), and Tangi Talo (c). The euhedral crystal shapes correspond with titanomagnetite of volcanic origin.

as mentinued before, the secondary magnetization was easily removed at an AF demagnetization between 5 to 20 mT, while Characteristics Remanent Magnetizations (ChRMs) could be isolated at peaks of 30 - 50 mT.

All the ChRMs are either progressing to the origin of the orthogonal vector projections or can be defined as the mean vectors that are stable in the intensity upon a higher AF demagnetization.

Fisher statistics for group mean directions for each sampled layer are provided in Table 1 and the equal area projection is shown in Figure 8. Although some points are scattered, two groups

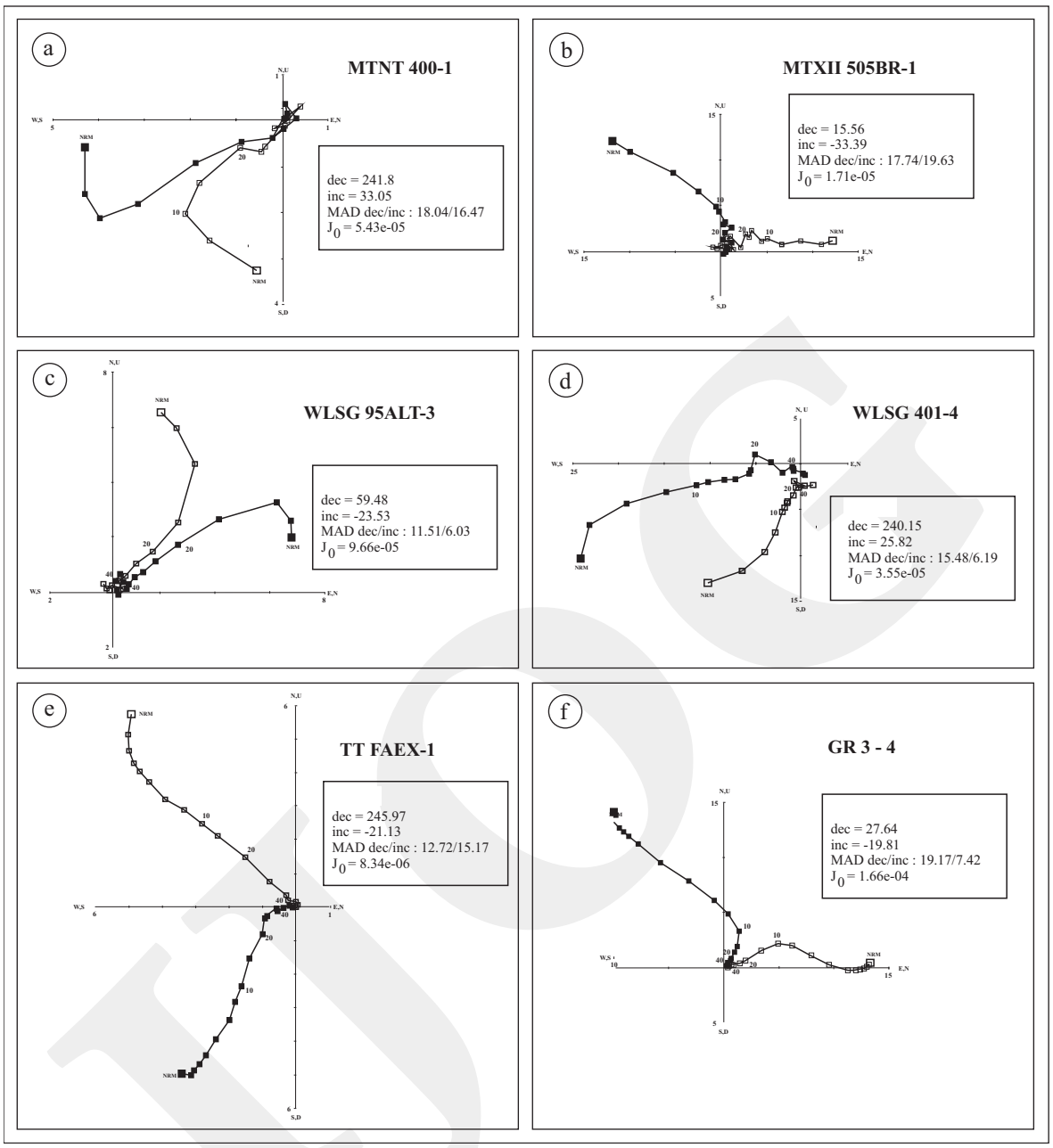

Figure 7. Representative progressive Zijderveld demagnetization diagrams (Orthogonal planes) of samples from Mata Menge (a, b), Wolo Sege (c, d), Tangi Talo (e), and Gero (f).

of opposite polarities can be easily recognized, and they all passed the reversal test as marked by the overlap of the normal α95 circle with the antipode of the reverse α95 circle (grey ghost circle) (Butler, 1998).

The McFadden & McElhinney reversal test is also passed, where the observed angle (γ_o) is not exceeding the critical angle (γ_c) (16.41º to 18.69º) and is classified as a "C" class according to McFadden & McElhinney (1990).

The grouping of the points, both normal and reverse, are better after demagnetization and the normal polarity group has slightly moved away from the present magnetic direction after demagnetization. One possibility is that some samples were strongly affected by the secondary magnetic field.

N represents the number of specimens analyzed per layer, although no firm criteria exist for acceptability of palaeomagnetic data . Within

Tabel 1. Magnetic intensities and Characteristic Remanent Magnetization Directions (ChRMs) for sampled layers in the So'a Basin. N represents the number of specimens analyzed per layer, R represents resultant vector, κ represents the dispersion of the direction population and α95 represents the confidence limit. Although no firm criteria exist for acceptability of palaeomagnetic data. Within-site κ > 30 and α95 values of <15 are generally considered to indicate reliable directions (Butler, 1998)

No	Samples ID	Intensity (A/m)		Remanent Direction		N	R	κ	α95
		Before Demagnetization	After Demagnetization	Mean Declination	Mean Inclination				
1	MTXII 90	2.27E-05	2.35E-07	50.2	-9.7	3	2.96	46.95	18.2
2	MTXII 260	1.06E-05	2.04E-07	77.5	34.7	5	4.76	16.93	19.1
3	MTXII 60 BR	6.92E-04	7.09E-06	21.2	0.5	4	3.9	31.31	16.7
4	MTXII 120 BR	7.32E-04	6.67E-06	8.9	-5.9	4	3.98	180.7	6.9
5	MTXII 265 BR	1.60E-04	4.98E-06	13.7	-4.1	5	4.53	8.52	27.8
6	MTXII 340 BR	9.82E-05	4.29E-06	31.7	-15.5	5	4.82	21.91	16.7
7	MTXII 505 BR	1.37E-05	1.06E-06	24	-15.9	5	4.86	29.59	14.3
8	MTXII 1318	1.06E-05	6.35E-07	24.4	-6.7	4	3.92	272.2	5.6
9	Mata 180	2.01E-04	6.87E-06	41.1	-13.3	4	3.95	57.06	12.3
10	Mata 220	4.21E-05	4.07E-06	22.7	-26.7	4	3.84	18.34	22
11	MTNT 230	4.76E-05	1.36E-06	59.3	-31.2	3	2.76	2.72	97.3
12	MTNT 270	6.52E-06	4.24E-07	57.5	5.3	4	3.9	31.31	16.7
13	MTNT 400	9.13E-05	3.82E-06	277.7	27.6	5	4.84	24.61	15.7
14	MTNT 500	1.08E-04	7.43E-06	206.1	23.9	4	3.74	11.76	28
15	MTNT 7C	2.29E-04	3.40E-05	29.9	-32.6	5	4.08	12.55	22.5
16	MTNT IGN 73	7.81E-04	9.59E-06	63.6	-21.5	5	4.36	6.21	33.4
17	MTNT MUD	2.70E-03	9.37E-05	210.8	32.9	4	3.96	77.8	10.5
18	WLSG 328	1.51E-04	6.53E-06	70.3	7	4	3.99	272.2	5.6
19	WLSG 401	3.38E-05	1.76E-06	232	28.3	4	3.97	111.9	8.7
20	WLSG 95 ALT	1.12E-04	6.74E-06	59.5	-23.4	4	3.99	559	3.9
21	WLSG 745	1.92E-04	1.42E-06	39.3	-22	5	4.96	105.8	7.5
22	TT 2.5	1.56E-04	1.02E-06	30.8	-31.3	4	3.89	26.33	18.2
23	TT 50a2010	3.44E-04	2.61E-06	228.2	1.8	5	4.79	19.18	17.9
24	TT 2000	2.79E-05	3.57E-06	249.9	38.8	3	2.94	31.04	22.5
25	TT 2116	6.99E-05	5.01E-06	235.7	53.7	4	3.8	14.94	24.6
26	TT FA excav	6.86E-06	4.53E-07	248.3	-6.3	4	3.71	10.28	30.1
27	TT 10 BFA	2.13E-06	5.36E-08	260.8	1.5	5	4.8	19.99	17.5
28	TT 2406	1.91E-05	5.54E-06	235	-12.1	5	4.96	110.1	7.3
29	GR 3	1.98E-04	4.19E-06	25.9	-28.1	5	4.83	23.94	16

site κ >30 and α 95 values of <15 are generally considered to indicate reliable directions (Butler, 1998).

The Magnetostratigraphy of the So'a Basin

Figure 9 shows the sampled stratigraphic sections from the So'a Basin together with the

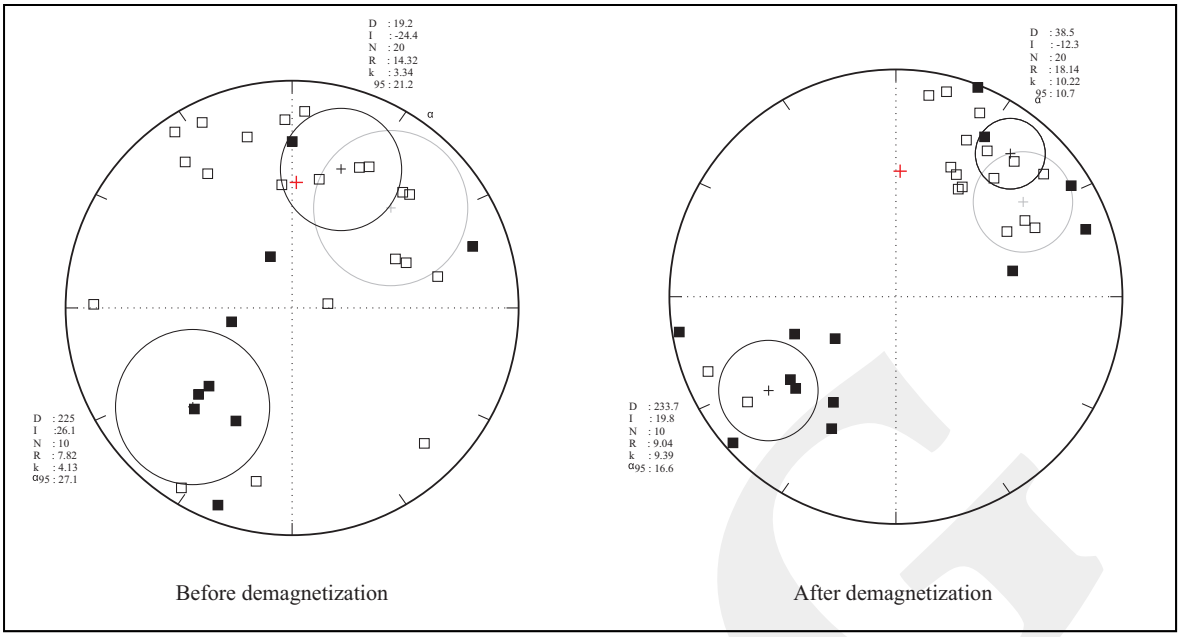

Figure 8. The equal area projection of individual mean directions obtained from the sampled levels of the So'a Basin. Open and solid squares in the equal area projections represent the upper and lower hemisphere, respectively. The black circles with centred crosses represent the mean magnetization directions (α95 circle) of normal (northern direction) and reverse (southern direction) polarities. Grey ghost circles represent the antipodes of the reverse α95 circles. A red cross represents the present-day magnetization direction.

magnetic polarities. Each section is plotted according to their relative topographic elevations, with Gero section being the highest and Tangi Talo the lowest. There are also the polarity correlations between sections and the composite litho- and magneto- stratigraphy as compared with the Standard Geomagnetic Polarity Time Scale (GPTS).

A total of four polarity magnetozones have been recognized in the So'a Basin. At the Mata Menge excavation section, all four magnetozones were recovered, which consist of two reverses (R1 and R2) and two normal (N1 and N2) zones. At the Wolo Sege trench section, there are two normals (N1 and N2) and one reverse (R2) zone. At the Tangi Talo trench section, two magnetozones can be recognized, which consist of one Reverse (R1) and one Normal (N1) zone, whereas at the much shorter Gero trench section, only one magnetozone was found (N2).

N1 is associated with the WSI. The numerical $^{40}Ar/^{39}Ar$ date of 1.02 Ma ± 0.2 for the WSI (Brumm *et al.,* 2010) indicates that N1 corresponds with the Jaramillo subchron on the GPTS. Furthermore, N2 at Mata Menge coincides with the sequence that is dated at ~0.8 – 0.5 Ma, and therefore correspond with the normal polarity of the Brunhes Chron. As the event/subchron of the N1 and N2 magnetozones is known, R1 and R2 can be inferred to correspond with the reverse polarity of Matuyama Chron (Figure 9).

The fossil bearing level at Tangi Talo (F3 in Figure 9) is situated below the lower boundary of the N1 magnetozone (Jaramillo) and it resulted in the relative age of > 1.07 Ma. It is difficult to determine the maximum age of this fossil layer, because the other subchrons are below the Jaramillo, such as the Cobb Mountain Event (1.24 – 1.22 Ma) or the Gilsa Event (1.68 Ma) were not recognized, which is not surprising since the sampling density in this interval is very low. Denser sampling in the future may reveal these events and allow a higher resolution in the oldest part of the So'a Basin sequence. However, this fossil layer probably will not exceed the bottom boundary of the Olduvai subchron (1.95 Ma), because a sample from the Ola Kile Formation, the top of which lies at ~2 m below the lowest

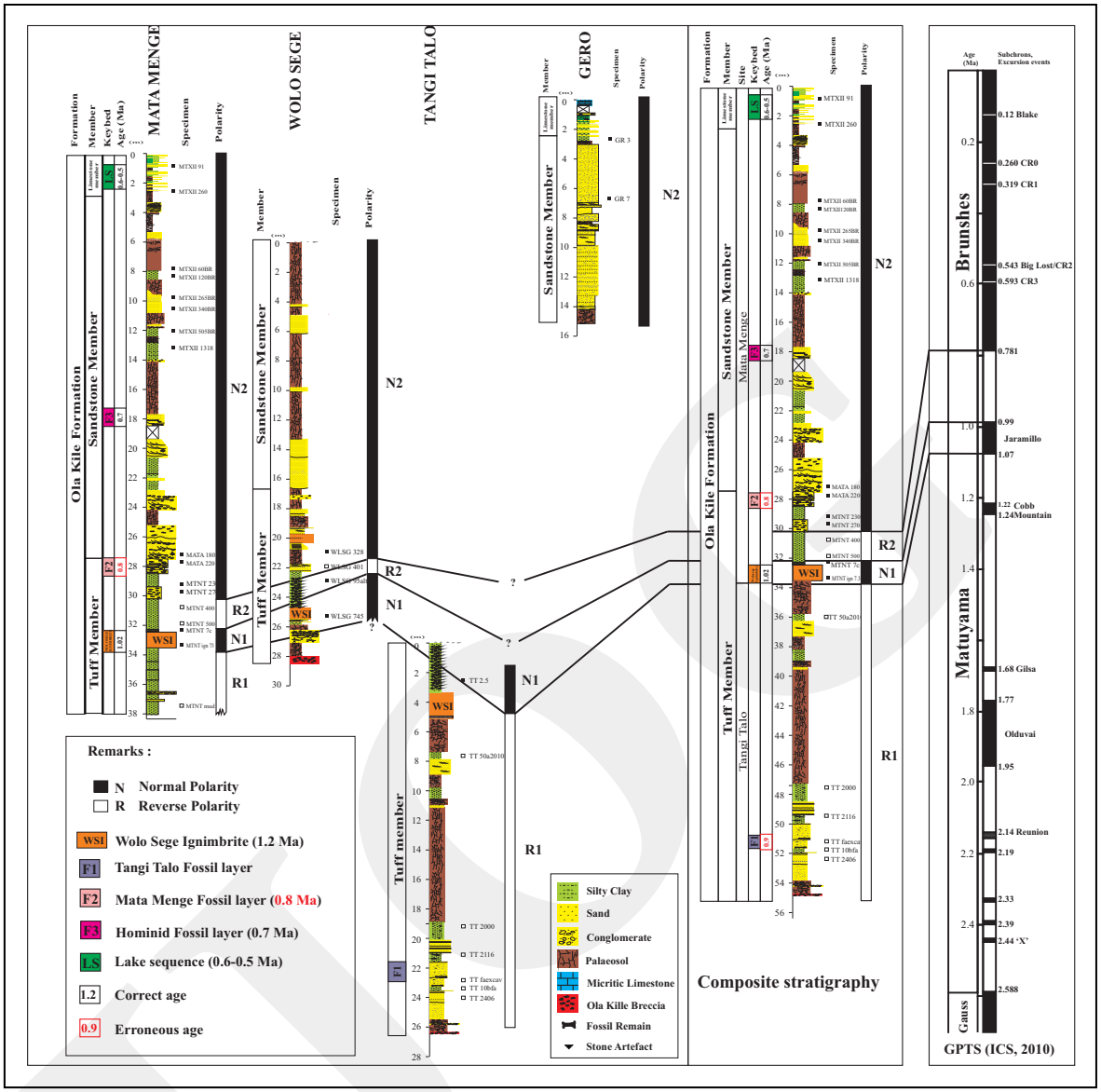

Figure 9. Magnetostratigrahy of the So'a Basin compared with radiometric dating results and the Standard Geomagnetic Polarity Time Scale [Geomagnetic Polarity Time Scale (GPTS), 2016]. Declination and inclination are the averages of the higher coercivity stable magnetization (ChRM). Black squares represent Normal Polarities and white squares represent Reverse Polarities.

Reverse sample in the Tangi Talo section, was dated at 1.8 Ma based on FT dating (O'Sullivan *et al*., 2001).

The two fossiliferous intervals in the Mata Menge section (F2 and F3 in Figure 9) are located above the boundary between R2 and N2. The lower (F2) and the upper (F3) are situated about 2.5 m and 12 m above the R2-N2 boundary, respectively. This means that those fossil layers are located above the boundary of Matuyama event (R2) and Brunhes event (N2) which means that both of them are younger than ~0.781 Ma.

These palaeomagnetic dating results have implications for the previous age estimates of fossil assemblages from the So'a Basin.

Firstly, palaeomagnetic dating of the Tangi Talo section combined with the $^{40}Ar/^{39}Ar$ dates given by Brumm *et al.* (2010) indicates that the Tangi Talo fossil-bearing level is older than previously thought. Instead of 0.9 Ma it now appears to be older than 1.07 Ma. Secondly, palaeomagnetic

dating has also confirmed the estimated age of the hominin remains, which were assumed to be ~0.7 Ma old (Brumm *et al.*, 2016). This estimation matches the palaeomagnetic dating result of Mata Menge section, which indicates that the hominin layer (F3) is younger than ~0.781 Ma. In addition, the palaeomagnetic results also show that previous age estimates for the lower fossil-bearing interval at Mata Menge (0.8 - 0.88 Ma; see O'Sullivan *et al.*, 2001) were slightly too old, and should be considered as minimal ~0.781 Ma.

Conclusion

Palaeomagnetic dating in the So'a Basin has recovered four polarity magnetozones. These magnetozones, from old to young, are as follows: R1 corresponds with the Matuyama Chron below the Jaramillo subchron; N1 with the Jaramillo subchron; R2 with the Matuyama Chron between the Jaramillo subchron, and the Brunhes Chron; and N2 with the Brunhes Chron.

These palaeomagnetic dating results support and refine the previously published radiometric ages related to the palaeontological and/or archaeological sites of the So'a Basin. The Tangi Talo fossil layer is situated below the bottom boundary of the Jaramillo. This provides a relative minimum age of > 1.07 Ma for the Tangi Talo fossil fauna, which is older than previously thought. Furthermore, two fossil intervals occurring in the Mata Menge section are located above the Matuyama-Brunhes boundary, which indicates that they are younger than 0.781 Ma.

However, it is necessary to propose additional studies with high resolution sampling interval in the studied area, in order to obtain a complete and the more appropriate stratigraphic age succession data.

Acknowledgements

This research project was financially supported by the Australian Research Council (ARC) Discovery grant (DP1093342) awarded to Michael. J. Morwood and Adam Brumm. The authors would like to acknowledge Gerrit van den Bergh and Brad Pillans for assessment and academic discussion of this project. The authors are also grateful to the former Heads of the Geological Agency, Surono and Ego Syahrial, the successive Directors of Centre for Geological Survey, A. D. Jumarma, Agung Pribadi, and Muhammad Wafid for permission to undertake this project. In addition, the acknowledgements are due to Iwan Kurniawan, Erick Setyabudi, and Wiji for their technical support during fieldwork, David Heslop for a support in the ANU rock magnetic laboratory, and Juju Jumbawan in the CGS SEM laboratory.

References

Ao, H., An, Z., Dekkers, M.J., Li, Y., Xiao, G., Zhao, H., and Qiang, X., 2013. Pleistocene magnetochronology of the fauna and Paleolithic sites in Nihewan Basin: Significance for environmental and hominin evolution in North China. *Quaternary Geochronology,* 18, p.78-92. DOI: 10.1016/j.quageo.2013.06.004

Aziz, F., van den Bergh, G.D., Morwood, M.J., Hobbs, D.R., Kurniawan, I., Collins, J., and Jatmiko. 2009. Excavation at Tangi Talo, central Flores, Indonesia. *In*: Aziz, F., Morwood, M.J., and Bergh, G. D. van (eds.), *Palaeontology and archaeology of the So'a Basin, central Flores, Indonesia*. Indonesian Geological Survey Institute, Bandung, p.1-18.

Brown, P. and Maeda, T., 2009. Liang Bua Homo floresiensis mandibles and mandibular teeth: a contribution to the comparative morphology of a new hominin species. *Journal of Human Evolution* 57, p.571-596. DOI: 10.1016/j.jhevol.2009.06.002

Brumm, A., Jensen, G.M., van den Bergh, G.D., Morwood, M.J., Kurniawan, I., Aziz, F., and Storey, M., 2010. Hominins on Flores, Indonesia, by one million years ago. *Nature*, 464, p.748-752. DOI:10.1038/nature08844.

Brumm, A., van den Bergh, G. D., Storey, M., Kurniawan, I., Alloway, B. V., Setiawan,

R., Setiyabudi, E., Grün, R., Moore, M. W., Yurnaldi, D., Puspaningrum, M. R., Wibowo, U. P., Insani, H., Sutisna, I., Westgate, J. A., Pearce, N. J. G., Duval, M., Meijer, H. J. M., Aziz, F., Sutikna, T., van der Kaars, S., Flude, S., and Morwood, M. J., 2016. Age and context of the oldest known hominin fossils from Flores. *Nature,* 534, p.249-253. DOI: 10.1038/nature17663

Butler, R. F., 1998. *Paleomagnetism: magnetic domains to geologic terrains*. Blackwell Scientific Publications, Boston. 238pp.

Dunlop, J. D., 2002. Theory and application of the Day plot (M_{rs}/M_s versus H_{cr}/H_c) 2. Application to data for rocks, sediments, and soils. *Journal of Geophysical Research,* 107 (B3), p.1-22. DOI: 10.1029/2001jb000487

Fisher, R.A., 1953. Dispersion on a sphere. *Proceedings of the Royal Society of London*. Series A, 217, p.295-305.

Geomagnetic Polarity Time Scale (GPTS), 2016. *International Commission on Stratigraphy*. http://www.stratigraphy.org/index.php/ics-chart-timescale. Accessed October 29, 2018.

Hartono, H. M. S., 1961. *Geological investigation at Olabula, Flores*. Djawatan Geologi, Bandung, 40pp.

Herries, A.I.R., Hopley, P., Adams, J., Curnoe, D., and Maslin, M., 2010. Geochronology and palaeoenvironments of the South African early hominin bearing sites. *American Journal of Physical Anthroplogy,* 143, p.640-646. DOI: 10.1002/ajpa.21389

Hounslow, M.W., 2006. PMagTools version 4.2- a tool for analysis of 2-D and 3-D directional data. http://dx.doi.org/10.13140/RG.2.2.19872.58880.

Hyodo, M., Watanabe, N., Sunata, W., Susanto, E. E., and Wahyono, H., 1993. Magnetostratigraphy of hominid fossil bearing formations in Sangiran and Mojokerto, Java. *Anthropological Sciences,* 101 (2), p.157-186. DOI: 10.1537/ase.101.157

Hyodo, M., Matsu'ura, S., Kamishima, Y., Takeshita, Y., Kitaba, I., Danhara, T., Aziz, F., Kurniawan, I., and Kumai, H., 2011. *High-resolution record of the Matuyama-Brunhes transition constrains the age of Javanese Homo erectus in the Sangiran dome, Indonesia. Proceedings of the National Academy of Sciences of the United States of America,* 108 (49), p.19563-19568. DOI: 10.1073/pnas.1113106108

Kirschvink, J. L., 1980. The least-squares line and plane and the analysis of the palaeomagnetic data. *Geophysical Journal International,* 62 (3), p.699-718.

Kobayashi, K.,Kitazawa, K., Kanaya, T., and SAKAI, T., 1971. Magnetic and micropaleontological study of deep-sea sediments from the west-central equatorial Pacific. *Deep-Sea Research*, 18. p.1045-1057. DOI: 10.1016/0011-7471(71)90093-3

Lepre, C.J. and Kent, D.V., 2010. New magnetostratigraphy for the Olduvai Subchron in the Koobi Fora Formation, northwest Kenya, with implications for early Homo. *Earth and Planetary Science Letters*, *290*, p.362-374. DOI: 10.1016/j.epsl.2009.12.032

Lurcock, P. C. and Wilson, G.S., 2012. PuffinPlot: A versatile, user-friendly program for paleomagnetic analysis. *Geochemistry, Geophysics, Geosystems, p.* 13 (6) p.1-6. DOI: 10.1029/2012gc004098

McFadden, P. L. and McElhinny, M.W., 1990. A new fold test for palaeomagnetic studies. *Geophysical Journal International,* 279 (103), p.163-169.

McElhinny, W. and McFadden, P.L., 2000. Paleomagnetism: Continent and Ocean. *Academic Press*, San Diego, 386pp.

Morwood, M. J., O'Sullivan, P.B., Aziz, F., and Raza, A., 1998. Fission-track ages of stone tools and fossils on the east Indonesian island of Flores. *Nature,* 392, p.173-176. DOI: 10.1038/32401

Murouka, H., Nasution, A., Urai, M., Takashi, M., Takashima, I., Simanjuntak, J., Sundhoro, H., Aswin, D., Nanlohy, F., Sitorus, K., Takahashi, H., and Kosek, T., 2002. Tectonic, volcanic, and stratigraphic geology of the Bajawa geothermal field, central Flores, Indonesia. *Bulletin of Geological Survey of Japan,* 53, p.109-138. DOI: 10.9795/bullgsj.53.109

Muttoni, G., Scardia, G., Kent, D. V., Swisher, C. C., and Manzi, G., 2009. Pleistocene magnetochronology of early hominin sites at Ceprano and Fontana Ranuccio, Italy. *Earth and Planetary Science Letters,* 286, p.255-268. DOI: 10.1016/j.epsl.2009.06.032

O'Sullivan, P., Morwood, M.J., Hobbs, D., Aziz, F., Suminto, and Situmorang, M. 2001. Archaeological implications of the geology and chronology of the So'a Basin, Flores, Indonesia.*Geology,* 29 (79), p.607-610. DOI: 10.1130/0091-7613(2001)029%3C0607:aiotga%3E2.0.co;2

Roberts, A. P., Cui, Y., and Verosub, K. L., 1995. Wasp-waisted hysteresis loops: Mineral magnetic characteristics and discrimination of components in mixed magnetic systems. *Journal of Geophysical Research,* 100, p.17,909-17,924. DOI: 10.1029/95jb00672

Shimizu,Y., Mubroto, B., Siagian, H., and Untung, M., 1985. A paleomagnetic study in the Sangiran area. Quaternary Geology of the Hominid Fossil Bearing Formations in Java. *In*: Watanabe, N. and Kadar, D. (eds.), *Geological Research and Development Centre, Special Publication,* 4, p.275-308.

Sondaar, P. Y., van den Bergh, G.D, Mubroto, B., Aziz, F., de Vos, J., and Batu, U.L., 1994. Middle Pleistocene faunal turnover and colonization of Flores, Indonesia by *Homo erectus*. *Human Paleontology*, p.1255-1262.

Suminto, Morwood, M. J., Kurniawan, I., Aziz, F., van den Bergh, G. D., and Hobbs, D. R., 2009. Geology and fossil sites of the So'a Basin, central Flores, Indonesia. *In*: Aziz, F., Morwood, M.J., and Bergh, G. D. van (eds), *Palaeontology and archaeology of the So'a Basin, central Flores, Indonesia.* Indonesian Geological Survey Institute, Bandung. p.19-40. DOI: 10.1130/0091-7613(2001)029%3C0607:aiotga%3E2.0.co;2

Tamrat, E., Thouveny, N., Taieb, M., and Brugal, J.P. 2014. Magnetostratigraphic study of the Melka Kunture archaeological site (Ethiopia) and its chronological implications. *Quartenary International,* 343. p.5-16. DOI: 10.1016/j.quaint.2013.11.030

Tauxe, L., 2003. *Paleomagnetic principles and practice*. Kluwer academic publisher. New Jersey, USA, 314pp.

van den Bergh, G. D., 1999. The Late Neogene elephantoid-bearing faunas of Indonesia. *Scripta Geologica,* 117, 388pp.

van den Bergh, G.D, Kurniawan, I., Morwood, M.J., Lentfer, C.J., Suyono., Setiawan, R., Aziz, F. 2009. Environmental reconstruction of the Middle Pleistocene archaeological/palaeontological site Mata Menge, Central Flores, Indonesia. *In*: Pleistocene Geology, paleontology and archaeology of the So'a basin, Central Flores, Indonesia. *Special Publication Centre for Geological Survey*, Indonesia. p.59-81

van den Bergh, G.D. 2010. 2010 So'a Basin field report. University of Wollongong. Unpublished.

van den Bergh, G. D., Kaifu, Y., Kurniawan, I., Kono, R.T., Brumm, A., Setiabudi, E., Aziz, F., and Morwood, M.J., 2016a. *Homo floresiensis*-like fossils from the early Middle Pleistocene of Flores. *Nature,* 534, p.245-248. DOI: 10.1038/nature17999

van den Bergh, G. D., Li, B., Brumm, A., Grün, R., Yurnaldi, D., Moore, M. W., Kurniawan, I., Setiawan, R., Aziz, F., Roberts, R. G., Suyono., Storey, M., Setiabudi, E., and Morwood, M. J. 2016b. Earliest occupation of Sulawesi, Indonesia. *Nature,* 529, p.208-211. DOI: 10.1038/nature16448

Zeeden, C., Hambach, U., Steguweit, L., and Anghelinu, M., 2009. Loess stratigraphy using palaeomagnetism: Application to the Poiana Cireşului archaeological site, Romania. *Quaternary International,* 240, (1-2), p.100-107. DOI: 10.1016/j.quaint.2010.08.018

Zijderveld, J. D. A., 1967. "A. C. Demagnetization of Rocks: Analysis of Results." *In*: Collinson, D. W., Creer, K. M., and Runcorn, S. K. (eds.), *Methods in Palaeomagnetism*, Elsevier, Amsterdam, New York, p.254-286.

Zuo, T.W., Cheng, H.J., Liu, P., Xie, F., and Deng, C.L., 2011. Magnetostratigraphic dating of the Hougou Paleolithic site in the Nihewan Basin, North China. *Science in China,* 54. p.1643-1650. DOI: 10.1007/s11430-011-4221-2